

Observational Properties of Proto-planetary Disk Gaps

Peggy Varnière¹, J. E. Bjorkman², Adam Frank¹, Alice C. Quillen¹, A. C. Carciofi²,
Barbara A. Whitney³, and Kenneth Wood⁴

ABSTRACT

We study the effects of an annular gap induced by an embedded proto-planet on disk scattered light images and the infrared spectral energy distribution (SED). We find that the outer edge of a gap is brighter in the scattered light images than a similar location in a gap-free disk. The stellar radiation that would have been scattered by material within in the gap is instead scattered by the disk wall at the outer edge of the gap, producing a bright ring surrounding the dark gap in the images. Given sufficient resolution, such gaps can be detected by the presence of this bright ring in scattered light images. For planets within 10 AU from the central star, the bright ring will be detectable only by next generation instruments, so we also briefly discuss the case of a planet farther out in the disk and its potential detection by existing instruments.

A gap in a disk also changes the shape of the SED. Radiation that would have been absorbed by material in the gap is instead reprocessed by the outer gap wall. This leads to a decrease in the SED at wavelengths corresponding to the temperature at the radius of the missing gap material and a corresponding flux increase at longer wavelengths corresponding to the temperature of the outer wall. We note that, unlike an inner hole in the disk, the presence of an annular gap does not change the bolometric IR flux; it simply redistributes the radiation, previously produced by material within the gap, to longer wavelengths. This implies that the changes in the SED generally will be smaller for gaps than holes. Although it will be difficult on the basis of the SED alone to distinguish between the presence of a gap and other physical effects, the level of changes can be sufficiently large to be measurable with current instruments (e.g., Spitzer).

¹Department of Physics & Astronomy, Rochester University, Rochester NY 14627-0171; pvarni@pas.rochester.edu; aquillen@pas.rochester.edu; afrank@pas.rochester.edu.

²Ritter Observatory, MS 113, Department of Physics and Astronomy, University of Toledo, Toledo, OH 43606-3390; jon@physics.utoledo.edu; acarcio@physics.utoledo.edu.

³Space Science Institute, 3100 Marine Street, Suite A353, Boulder, CO 80303; bwhitney@colorado.edu.

⁴School of Physics & Astronomy, University of St Andrews, North Haugh, St Andrews, Fife, KY16 9AD, Scotland the Brave; kw25@st-andrews.ac.uk.

Subject headings: Stars: Planetary Systems: Protoplanetary Disks — Stars: Circumstellar Matter — Stars: Pre-main-sequence — Infrared: Stars — Radiative Transfer — Hydrodynamics

1. Introduction

Inner holes in protostellar and planetary debris disks surrounding young stars have been detected through the study of their spectral energy distributions (Koerner, Sargent, & Beckwith 1993; Jura et al. 1998; Calvet et al. 2002; Rice et al. 2003) and confirmed, in some cases, by direct images (Koerner et al. 1998; Jayawardhana et al. 1998; Weinberger et al. 1999; Schneider et al. 1999). Additionally, warm optically thin gas in the cleared region may be responsible for the observed CO line emission in T Tauri stars (Najita, Carr, & Mathieu 2003).

The presence of such holes has been suggested to be evidence that planets have formed in these systems (Strom, Edwards, & Skrutskie 1993). When planets form in the protostellar disk, they initially sweep up the material in their vicinity, tidally clearing gaps in the disk (Lin & Papaloizou 1986). Ultimately as accretion stops, the disk dissipates creating a large central hole (see Hollenbach, Yorke, & Johnstone 2000 for a discussion of possible mechanisms). Since gaps and holes in protostellar disks arise through the gravitational interaction between the disk and planets, detailed studies of the emission from disks containing planets may allow us to place constraints on the properties of the embedded planets and on the evolution of these systems.

Most previous work has investigated the effects of holes rather than gaps and assumed that the hole or gap simply causes a reduction in the flux at a particular wavelength due to the lack of dust at the equilibrium temperatures within the hole (e.g., Hillenbrand et al. 1992) or gap (Boss & Yorke 1996; Beckwith 1999). However, the gap is vertically extended, so one must also account for the walls of the gap. Initial studies that included some of these 3-D radiative transfer effects were performed by Wolf et al. (2002); Wolf & D’Angelo (2005) who combined the results of 2-D hydrodynamics simulations with a 3-D Monte Carlo radiative transfer code to explore the observational consequences of a planetary gap. Since Wolf et al. (2002); Wolf & D’Angelo (2005) were primarily interested in detecting the disk density structures induced by the planet, they assumed the disk scale height, H/r , is independent of radius (i.e., an unflared disk) when converting the 2-D surface density from the hydrodynamics simulation into the vertically extended (3-D) density required by the radiative transfer model. However, as explored by Dullemond, Dominik, & Natta (2001) and Calvet et al. (2002), the inner wall of a vertically extended disk with a hole is directly illuminated

by the central star, which increases the temperature of the wall relative to the upper surface of the disk itself, producing a bright inner edge to the disk. A similar effect occurs when a gap is created in a *flared* disk.

Here we investigate the properties of illuminated gap edges and how they affect the infrared spectral energy distribution (SED) and morphology of scattered light images. In a flared disk, the outer wall of the gap intercepts and scatters radiation that normally would have been reprocessed within the gap. Thus the outer wall produces a bright ring surrounding the dark gap in the scattered light images — an effect not observed by Wolf et al. (2002) because they did not employ a flared disk. Similarly, the increased temperature of the outer wall increases the SED at intermediate wavelengths. To obtain SEDs and scattered light images, we coupled the output of 2-D hydrodynamics simulations of a disk/planet interaction (see, for example, Masset & Papaloizou 2003; Varnière, Quillen, & Frank 2004) to our 3-D Monte Carlo radiative transfer (MCRT) codes, assuming a flared disk geometry.¹ The SEDs were calculated using the radiative equilibrium method developed by Bjorkman & Wood (2001), as extended to T Tauri disks (Wood et al. 2002a, 2002b) and protostellar envelopes (Whitney et al. 2003). The scattered light images were calculated using the MCRT code developed by Whitney & Hartmann (1992) for young stellar object (YSO) disks. Subsequently, this scattered light code was modified to efficiently calculate images of complex 3-D YSO envelope geometries (Wood et al. 2001; Whitney & Wolff 2002).

2. Methods

Our previous work includes a numerical hydrodynamics study of the properties of disk edges that are maintained by giant planets (Varnière et al. 2004). The 2-D hydro simulations use a polytropic equation of state with $\gamma \approx 1$ to mimic the effects of strong cooling (reducing γ increases the internal degrees of freedom thereby increasing the compression behind shocks as would occur with strong cooling). In this work we use the results of two hydro simulations, consisting of 2-D gas surface density distributions, to compute synthetic scattered light images and SEDs using the MCRT codes.

Both simulations have the same initial conditions: a central star of mass $M_* = 1M_\odot$, radius $R_* = 2.5R_\odot$, effective temperature of 4.10^3K , and a gas disk extending from $0.1\text{ AU} < r < 10\text{ AU}$ with a Reynolds number ($\mathcal{R} = 10^7$). We use an initial disk surface density profile $\Sigma(r) \propto 1/r$ and specify the normalization so that the total disk mass $M_d = 10^{-2}M_\odot$. The

¹We also have performed full hydrostatic equilibrium calculations of the disk vertical structure, but the results are essentially the same as the power law flared disk models.

first simulation has no planet and acts as a control. The second simulation contains a single two-Jupiter-mass-planet ($M_p = 2M_J$) in a circular orbit of radius 1 AU. We ran the simulations for 1000 orbits of the planet — long enough that the gap density attains its steady-state value.

We note that our simulated disks only extend to 10AU. To predict longer wavelength emission, we require a larger disk extent, so after the hydro simulations are performed, we artificially extend the gas surface density out to a disk radius of 300 AU using our $(1/r)$ initial density profile. Similarly, we extend the surface density to the disk inner radius r_i . The resulting surface density then is entered into the MCRT code.

The Monte Carlo radiation transfer code is fully 3-D, so we require an input 3-D disk density. To convert the 2-D disk surface density (from the hydro simulation), we assume the vertical structure of the disk is Gaussian with a scale height that varies as a power law with radius (i.e., a flared disk; see Whitney et al. 2003, section 2.1, for details). In the future, we hope that fully 3-D simulations of the disk will allow a more accurate treatment of the vertical disk structure. Finally for the dust opacity, we use the large dust grains that Wood et al. (2002b) found were required to fit the SED of HH30 IRS.

2.1. Scattered Light Images

In Figure 1, we present the scattered light images produced from the Monte Carlo simulations. Each image was created using 10^8 photons. Although the photons were propagated throughout the entire disk (out to 300AU), Figure 1 shows only the central 7×7 AU. The images at left show the simulations without a planet, while the images at right include a $2M_J$ planet located at 1AU. The width of the gap (where the density is significantly lowered) is about 1 AU. From top to bottom are shown two inclinations: an almost face-on system (5°) and a near edge-on (70°) system. As expected, the gap created by the planet also creates a gap in the scattered light images. Furthermore, the outer edge of the gap appears brighter compared to the same location in the control case.

To investigate the morphology and magnitude of the excess emission, we plot in figure 2 the azimuthally averaged surface brightness profile for a simulation with a planet at 1AU viewed face-on. This shows that the ring located at the outer gap edge has a surface brightness that is about four times as bright as the emission from the smooth disk at the same location. This excess emission is likely caused by the increased illumination of the outer wall of the gap by stellar photons that are no longer absorbed by disk material within the gap (recall that the disk scale height increases with radius, so the photons that would have been

absorbed in the gap now hit the outer vertical wall of the gap). We conclude that a bright ring surrounding a darker ring is a characteristic signature of a gap in a flared disk. This is in distinction to the solitary dark annulus that occurs when disk flaring is not included (see fig. 2 of Wolf et al. 2002). Consequently, we expect that the brightness of the ring might be used to measure the degree of disk flaring.

After the initial gap is created, the inner region of the disk eventually is cleared, producing an inner hole in the disk. Wolf & D’Angelo (2005) explored the transition between these phases (their model has both a gap and a partially cleared inner disk). Interestingly, despite the absence of flaring, they now find a bright ring surrounding a darker gap (see fig. 2 of Wolf & D’Angelo 2005). Most likely, this is because the inner region of their disk is optically thin, so the outer wall of the gap is now becoming the inner wall of the remaining disk (and inner walls directly illuminated by the star also produce bright rings). We conclude that a bright ring surrounding a dark gap will first occur (in scattered light images) as the protoplanet initially clears a gap. Then as the inner disk is cleared, the wall will become hotter as it begins to be directly illuminated by the star. Thus (in thermal emission images) the ring will become brighter as the inner hole develops.

We will now focus on the detectability of the gap itself. The size of the gap opened by a planet depends on the mass of the planet and its semi-major axis (Varnière et al. 2004). For a $2M_J$ planet at 1AU, the gap size is about 1 AU. Taking a typical gap of 1AU, for a system at 100 pc ($1'' = 100\text{AU}$), an angular resolution of $0.2''$ would allow a gap to be resolved for a Jupiter planet with $a \gtrsim 25\text{AU}$. An angular resolution of $0.02''$ would allow a gap to be resolved for planets with $a \gtrsim 2.5\text{AU}$. We conclude that the direct detection of planetary gaps in the inner regions of the disk will require the higher resolution of future instruments. Finally we note that radial velocity and transit searches, currently the principle means of planet detection, are biased against the detection of planets at large distances, making the direct imaging searches we propose here complimentary.

2.2. SED

Since current instruments can only detect gaps in the outer regions of the disk, we are also interested in the potential for an indirect detection of a planetary gap via its impact on the SED. Note, however, that SEDs generally are not unique since different physical effects can sometimes cause similar changes. This means that careful modeling of all available observations is required to limit the range of possibilities before one may conclude that a gap is the most likely origin of the changes in the SED. To study the effect of gaps on the SED, we have performed two additional sets of simulations. The initial conditions for the

first set of simulations places the planet close to the star at $r_p = 0.15 \text{ AU}$ with the inner edge of the disk located at the dust destruction radius, $r_i = 0.07 \text{ AU}$. The second set has a planet at $r_p = 5 \text{ AU}$ with the inner edge of the disk located at $r_i = 1 \text{ AU}$. In this later case, it is assumed that a second planet at $r < r_i$ has cleared out an inner hole. These two cases bracket the SED behavior we have observed from a larger set of runs covering a large range of parameters. For each set of simulations we calculated SEDs using two different dust models that comprise limiting cases: large dust grains used to successfully model HH30 (Wood et al. 2002b) and ISM dust (Kim, Martin, & Hendry 1994). Both models use a power law distribution of grain sizes from small to large (with an exponential cutoff). The primary difference is that the HH30 dust has a higher proportion of big grains.

To calculate the the infrared SED for each of our simulations, including the control simulations without a gap, we used the Monte Carlo radiative equilibrium code described by Whitney et al. (2003). The SEDs for four cases are displayed in Figure 3. The leftmost panels show the small hole models ($r_i = 0.07 \text{ AU}$, $r_p = 0.15 \text{ AU}$); the rightmost panels show the large hole models ($r_i = 1 \text{ AU}$, $r_p = 5 \text{ AU}$). Similarly, the upper panels employ ISM dust, while the lower panels use the large HH30 dust grains. Each plot compares the SED with a gap (solid line) to that of the control simulation without a gap (dashed line).

We focus first on the large hole ($r_i = 1 \text{ AU}$) model with large dust grains (lower right panel). Our results indicate that the presence of the gap reduces the emission between $\sim 5 \mu\text{m}$ and $\sim 20 \mu\text{m}$ as expected owing to the removal of the emission by warm dust in the gap. Around $8 \mu\text{m}$ the deficit is about 30% of the control simulation. Note, however, the presence of excess emission at longer wavelengths (from $\sim 20 \mu\text{m}$ to $\sim 100 \mu\text{m}$). At $25 \mu\text{m}$ this excess is of the order of 7% of the control simulation. This excess arises from the heating of the vertical disk wall at the outer edge of the gap. The heating occurs because the photons that would have been absorbed in the gap are reprocessed instead by the outer wall. Since this effect does not change the total luminosity reprocessed by the disk, the gap does not change the IR bolometric flux. Instead the gap causes the deficit to be redistributed to longer wavelengths, preserving the total area of the IR SED. One consequence of this redistribution is that gaps produce smaller changes in the SED than previous work suggested (compare Fig. 3 to Fig. 3 of Boss & Yorke 1996 and Fig. 4 of Beckwith 1999).

The conservation of IR bolometric flux is a primary factor that can distinguish gaps from inner disk holes. In the case of a small inner hole, changing the hole radius changes how much stellar radiation escapes through the hole. But for a large inner hole (one for which the star is effectively a point source), the situation is less clear; it depends on how the increase of disk radius, which removes material from the disk, alters the solid angle subtended by the optically thick region of the disk. In general, one expects that increases in hole radius will

decrease the fraction of starlight reprocessed by the disk. Thus holes with different radii will most likely have different IR bolometric fluxes. This implies that increasing the hole radius produces a flux deficit at short wavelengths without producing a correspondingly large flux increase at long wavelengths. In contrast, gaps of different radii (and widths) have the same IR bolometric flux, which also implies that gaps generally produce smaller changes in the SED than holes.

Although, in general, a gap redistributes the flux, the amount of redistribution (and hence detectability of the gap) depends sensitively on both the location of the gap and the hole radius (inner edge of the disk). For example, if the disk extends to small radii (left panels of Fig. 3), we find that emission from hot dust in the inner regions of the disk overwhelms and fills in the potential deficit caused by the gap. Similarly, the emission excess becomes too weak to be detected.

Even if the flux changes are large enough to be detected, it will be very difficult to conclude that a gap is responsible. For example, changes in the dust properties will alter the wavelength-dependence of the opacity, which can affect the shape of the SED. Comparing the top and bottom panels on the right side of Figure 3, we see that changing the dust size distribution produces changes in the mid-IR flux levels that are comparable in magnitude to those produced by a gap. Therefore, depending on the details of the dust opacity, it is quite possible that these changes could mimic the effects of a gap. Similarly, changing the disk scale height (by dust settling, for example) in combination with changing the hole radius could also alter the shape of the SED in ways that might mimic a gap. Such well-known degeneracies in the parameters of SED model fitting imply that it will be quite difficult to infer the presence of a gap on the basis of the SED alone.

3. Conclusion

We have studied the observational consequences of the presence of a gap in a protoplanetary disk using a Monte-Carlo radiative transfer code. Our results show that disk gaps appear as more than simply dark annuli in the images. The direct illumination by stellar photons of the vertical disk wall at the outer edge of the gap results in a dramatic brightening, thereby producing a characteristic bright ring around the dark gap in the scattered light images.

The detectability of the gap will depend on the inclination of the disk, the resolution of the detector, and on the size of the gap. Note that if the disk viscosity is higher than we considered here, the gap will be narrower and may contain more gas, making it more difficult

to identify in either a scattered light image or an SED.

Our results for the SEDs from disks with gaps show once again that the direct illumination and therefore heating of the outer gap wall can have measurable consequences (but only in favorable circumstances). We find both an emission excess (at longer wavelengths) due to the heating of the outer wall of the gap, as well as an emission deficit (at shorter wavelengths) due to the cleared region within the gap. Furthermore unlike an inner disk hole, the gap does not change the fraction of the stellar luminosity reprocessed by the disk, so the gap does not change the bolometric IR flux; it simply redistributes the flux from shorter to longer wavelengths. A consequence of this redistribution is that gaps will be harder to detect than inner holes. Nonetheless, the changes in the SED can be detected in some cases, but we caution that other physical effects, such as variations in the disk thickness, density distribution, and dust properties may change the SED in ways that mimic the presence of a gap. We conclude that detecting gaps on the basis of the SED alone in optically thick disks will be difficult, so the most likely method for unambiguously detecting the earliest stages of planet formation will be to observe a bright ring surrounding a dark gap in scattered light images.

This work was supported by the National Science Foundation: grants AST-0307686 (AC, JEB), AST-9702484 (AF), AST-0098442 (AF), AST-0406823 (AQ) NASA: grants NAG5-8794 (JEB), NAG5-8428 (AF), NNG04GM12G (AQ,AF) DOE grant DE-FG02-00ER54600 (AF), and the Laboratory for Laser Energetics.

REFERENCES

- Beckwith, S. V. W. 1999, in *The Origin of Stars and Planetary Systems*, ed. C. J. Lada & N. D. Kylafis (Dordrecht: Kluwer), 579
- Boss, A. P., & Yorke, H. W. 1996, *ApJ*, 469, 366
- Bjorkman, J. E., & Wood, K. 2001, *ApJ*, 554, 615
- Calvet, N., D'Alessio, P., Hartmann, L., Wilner, D., Walsh, A., & Sitko, M. 2002, *ApJ*, 568, 1008
- Dullemond, C. P., Dominik, C., & Natta, A. 2001, *ApJ*, 560, 957
- Hillenbrand, L. A., Strom, S. E., Vrba, F. J., & Keene, J. 1992, *ApJ*, 397, 613

- Hollenbach, D. J., Yorke, H. W., & Johnstone, D. 2002, in *Protostars and Planets IV*, ed. V. Mannings, A. P. Boss, & S. S. Russell (Tucson: Univ. Arizona Press), 401
- Jayawardhana, R., Fisher, S., Hartmann, L., Telesco, C., Pina, R., & Giovanni, F. 1998, *ApJ*, 503, L78
- Jura, M., Malkan, M., White, R., Telesco, C., Pina, R., & Fisher, R. S. 1998, *ApJ*, 505, 897
- Kim, S. H., Martin, P. G., & Hendry, P. D. 1994, *ApJ*, 422, 164
- Koerner, D. W., Sargent A. I., & Beckwith, S. V. W. 1993, *Icarus*, 106, 2
- Koerner, D. W., Ressler, M. E., Werner, M. W., & Backman, D. E. 1998, *ApJ*, 503, L83
- Lin, D. N. C., & Papaloizou, J. C. B. 1986, *ApJ*, 307, 395
- Masset, F. S., & Papaloizou, J. C. B. 2003, *ApJ*, 588, 494
- Najita, J., Carr, J. S., & Mathieu, R. D. 2003, *ApJ*, 589, 931
- Rice, W. K. M., Wood, K., Armitage, P. J., Whitney, B. A., & Bjorkman, J. E. 2003, *MNRAS*, 342, 79
- Schneider, G., et al. 1999, *ApJ*, 513, L127
- Strom, S. E., Edwards, S., & Skrutskie, M. F. 1993, in *Protostars and Planets III*, ed. E. H. Levy & J. I. Lunine (Tucson: Univ. Arizona Press), 837
- Varnière, P., Quillen, A. C., & Frank, A. 2004, *ApJ*, in press
- Weinberger, A. J., Becklin, E.E., Schneider, G., Smith, B. A., Lowrance, P.J., Silverstone, M.D., Zuckerman, B., & Terrile, R. J. 1999, *ApJ*, 525, L53
- Whitney, B. A., & Hartmann, L. 1992, *ApJ*, 395, 529
- Whitney, B. A., & Wolff, M. J. 2002, *ApJ*, 574, 205
- Whitney, B. A., Wood, K., Bjorkman, J. E., & Wolff, M. J. 2003, *ApJ*, 591, 1049
- Wolf, S., Gueth, F., Henning, T., & Kley, W. 2002, *ApJ*, 566, L97
- Wolf, S., D'Angelo, G. 2005, *ApJ*, 619, 1114
- Wood, K., Lada, C. J., Bjorkman, J. E., Kenyon, S. J., Whitney, B. A., & Wolff, M. J. 2002a, *ApJ*, 567, 1183

Wood, K., Smith, D., Whitney, B. A., Stassun, K., Kenyon, S. J., Wolff, M. J., & Bjorkman, K. S. 2001, *ApJ*, 561, 299

Wood, K., Wolff, M. J., Bjorkman, J. E., & Whitney, B. A. 2002b, *ApJ*, 564, 887

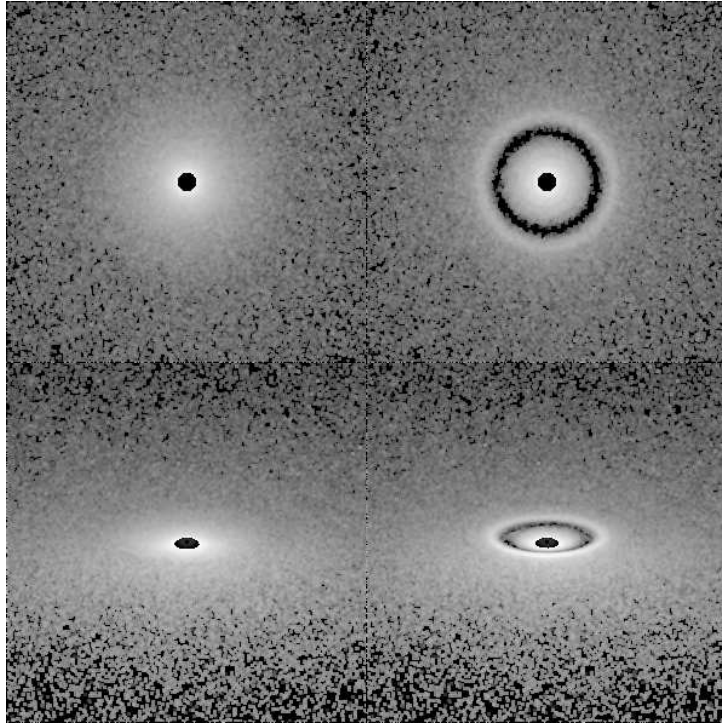


Fig. 1.— Model scattered light images. The top figures show the log of the optical disk surface brightness viewed at an inclination of $i = 5^\circ$. The bottom figures show disks viewed at $i = 70^\circ$. On the left there is no gap in the disk, on the right there is a gap created by a 2 Jupiter mass planet clearing a gap centered at 1 AU with a width of about 1AU. (Gap width defined via half-minimum depth of density in gap; Varnière et al. (2004)) The images show a region 7×7 AU.

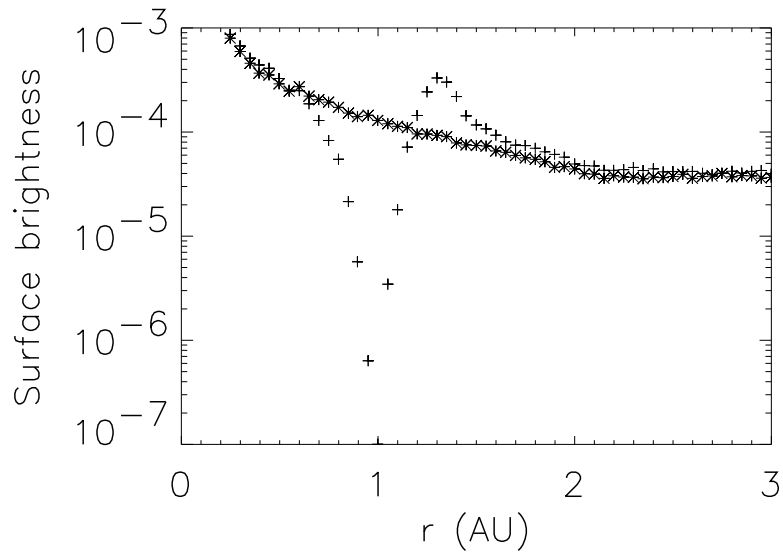


Fig. 2.— Comparison between the azimuthally averaged optical surface brightness profiles for two disks viewed face-on. One disk contains a 2 Jupiter mass planet at 1AU (shown as crosses) and the other lacks a planet (shown as starred points). The simulated disks are the same as those shown in Fig 1. The gap is seen as a decrease in the surface brightness profile near the planet. There is also a bump in the profile on the outer gap edge, corresponding to the bright ring seen in Fig. 1.

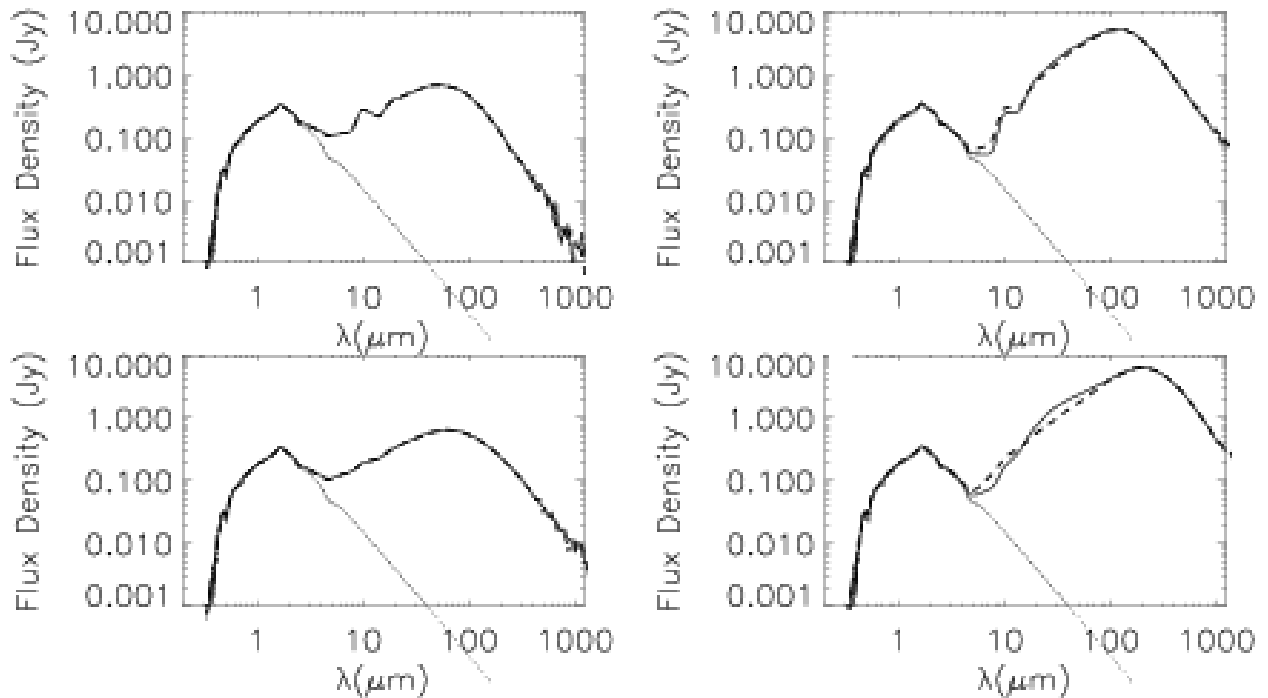


Fig. 3.— Spectral Energy Distributions. The spectral energy distributions for simulations containing a gap created by a $2M_J$ planet are shown (solid lines) in comparison to a control simulation lacking a planet (dotted lines). The left panels show the $r_p = 0.15 AU$, $r_i = 0.07 AU$ models, while the right panels show the $r_p = 5 AU$, $r_i = 1 AU$ models. In the top (bottom) panels, we show the results for the ISM (HH30) dust model.